

REPORT DOCUMENTATION PAGE				Form Approved OMB No. 0704-0188	
<small>The public reporting burden for this collection of information is estimated to average 1 hour per response, including the time for reviewing instructions, searching existing data sources, gathering and maintaining the data needed, and completing and reviewing the collection of information. Send comments regarding this burden estimate or any other aspect of this collection of information, including suggestions for reducing the burden, to Department of Defense, Washington Headquarters Services, Directorate for Information Operations and Reports (0704-0188), 1215 Jefferson Davis Highway, Suite 1204, Arlington, VA 22202-4302. Respondents should be aware that notwithstanding any other provision of law, no person shall be subject to any penalty for failing to comply with a collection of information if it does not display a currently valid OMB control number.</small> PLEASE DO NOT RETURN YOUR FORM TO THE ABOVE ADDRESS.					
1. REPORT DATE (DD-MM-YYYY) 01122001		2. REPORT TYPE Journal Article		3. DATES COVERED (From - To)	
4. TITLE AND SUBTITLE Concentration Gradient, Diffusion, and Flow Through Open Porous Medium Near Percolation Threshold via Computer Simulations				5a. CONTRACT NUMBER N0001402WX30005	
				5b. GRANT NUMBER N/A	
				5c. PROGRAM ELEMENT NUMBER 0601153N	
				5d. PROJECT NUMBER BE032-04-4D	
6. AUTHOR(S) R.B. Pandey, J.F. Gettrust, D. Stauffer				5e. TASK NUMBER	
				5f. WORK UNIT NUMBER 74-7814-00	
7. PERFORMING ORGANIZATION NAME(S) AND ADDRESS(ES) Naval Research Laboratory Marine Geoacoustics Division Stennis Space Center MS 39529				8. PERFORMING ORGANIZATION REPORT NUMBER NRL/JA/7430--01-9	
9. SPONSORING/MONITORING AGENCY NAME(S) AND ADDRESS(ES) Office of Naval Research 800 North Quincy Street Arlington VA 22217-5000				10. SPONSOR/MONITOR'S ACRONYM(S) ONR	
				11. SPONSOR/MONITOR'S REPORT NUMBER(S)	
12. DISTRIBUTION/AVAILABILITY STATEMENT Approved for public release; distribution is unlimited					
13. SUPPLEMENTARY NOTES Physica A (2001) Volume 300 Pg. 1					
14. ABSTRACT Abstract: The interacting lattice gas model is used to simulate fluid flow through an open percolating porous medium with the fluid entering at the source-end and leaving from the opposite end. The shape of the steady-state concentration profile and therefore the gradient field depends on the porosity (p). The root mean square (rms) displacements of fluid and its constituents (tracers) show a drift power-law behavior.					
15. SUBJECT TERMS Lattice gas; Fluid flow; Percolating; Porous medium; Gradient field					
16. SECURITY CLASSIFICATION OF:			17. LIMITATION OF ABSTRACT SAR	18. NUMBER OF PAGES 19	19a. NAME OF RESPONSIBLE PERSON Ras Pandey
a. REPORT Unclassified	b. ABSTRACT Unclassified	c. THIS PAGE Unclassified			19b. TELEPHONE NUMBER (Include area code) 228-688-5480

20020717 117

Concentration Gradient, Diffusion, and Flow Through Open Porous Medium Near Percolation Threshold via Computer Simulations

R.B. Pandey^{1,2}, J.F. Gettrust¹, and D. Stauffer^{3,4}

¹Naval Research Laboratory
Stennis Space Center, MS 39529

²Department of Physics and Astronomy
University of Southern Mississippi, Hattiesburg, MS 39406-5046

³Instituto de Fisica
Universidade Federal Fluminense, Av. Litoranea s/n, Boa Viagem
Niteroi 24210-340, RJ, Brazil

⁴Institute for Theoretical Physics
Cologne University, D-50923 Köln, Euroland

Abstract: The interacting lattice gas model is used to simulate fluid flow through an open percolating porous medium with the fluid entering at the source-end and leaving from the opposite end. The shape of the steady-state concentration profile and therefore the gradient field depends on the porosity (p). The root mean square (rms) displacements of fluid and its constituents (tracers) show a drift power-law behavior, $R \propto t$ in the asymptotic regime ($t \rightarrow \infty$). The flux current density (j) is found to scale with the porosity according to, $j \propto (\Delta p)^\beta$ with $\Delta p = p - p_c$ and $\beta \simeq 1.7$.

PACS numbers: 05.10.Ln; 05.40.-a; 0.5.60.Cd; 47.55.Mh; 83.85.Pt

1 Introduction

Motion of fluid/gas constituents (tracers) determines the collective diffusion of fluid/gas concentration. In general, tracers movements are correlated and depend on the concentration of fluid and the porosity of host medium/matrix among other parameters such as temperature, interaction, pressure gradient, etc. Using a computer simulation model involving the interacting lattice gas, we consider the flow of fluid through a percolating porous medium [1] near its percolation threshold at a fixed temperature. It involves the motion of constituents, global transport of fluid, evolution of concentration profile in unsteady-flow, concentration gradient and flux rate in steady-state flow. A brief introduction and remark on some of these issues may help understanding our data. We simulate the flow through random walks (stochastic motion of each particle), but in contrast to many previous such diffusion studies we create a net flow by continuously injecting new particles at the bottom, thus forcing the already existing ones to move upwards since no two particles can occupy the same lattice site. The system thus is spatially inhomogeneous in vertical direction.

1.1 Concentration diffusion

Diffusion of fluid concentration (C) in a homogeneous space is described by

$$\frac{\partial C}{\partial t} = D_m \nabla^2 C \quad . \quad (1)$$

Evolution of the concentration profile, diffusion of its front in unsteady flow, and drift in steady-state flow regimes are well understood [2]. How does the concentration diffuse (i.e., fluid flow) in a porous medium [3] such as percolating system [4-6]? What type of motion do the fluid and its constituents exhibit in unsteady and steady-state flow regimes? How does the flux-rate depend on porosity? Addressing these questions becomes somewhat difficult with respect to solving the diffusion equation (1) particularly near percolation threshold [7-9] where the percolating pores are highly ramified; the boundary conditions involved with the pore space become prohibitively large to solve the diffusion equation numerically. We consider an interacting lattice gas to model the fluid in order to address these questions in a percolating

porous matrix. The lattice gas consists of hard-core particles with a nearest neighbor interaction (see section 2).

1.2 Tracer: diffusion, subdiffusion, drift

A considerable progress has emerged in understanding the motion of a particle executing its random walk in percolating system [4,5]. Variation of the root mean square displacement (R) with time (t) is one of the major quantities to characterize the type of motion, i.e.,

$$R = A \cdot t^{\nu_1} + B \cdot t^{\nu_2} + \dots \quad (2)$$

If $\nu_1 > \nu_2$, then $R \simeq A \cdot t^{\nu_1}$ in the asymptotic time limit ($t \rightarrow \infty$). With such a leading power-law variation, the motion is diffusive if $\nu_1 = 1/2$ and drift if $\nu_1 = 1$. In a percolating system at porosity (the fraction of pore sites) above threshold, $p > p_c$, we have $\nu_1 = 1/2$. At the percolation threshold [7-9], on the other hand, the random walk motion becomes anomalous diffusion with $\nu_1 \simeq 0.2$ in three dimensions and $\nu_1 \simeq 0.3$ in two dimensions [10].

In presence of a biased field [11-13], the motion of a particle can still be described by above equation (2) except at very high bias with diffusion ($\nu_1 = 1/2$) in short time and drift ($\nu_2 = 1$) in the long time regime at $p \gg p_c$ with a crossover around $t = (A/B)^2$. The motion becomes very complex [11] as the porosity is reduced toward the threshold and the biased field competes with the barriers at the pore boundaries. The motion of a particle in such a porous medium has been extensively studied in a variety of biased fields for over a decade [11-17]. Many interesting findings have been reported particularly due to increased computing power. Some of these results include vanishing drift velocity above a characteristic or critical field [13,15], sub-diffusion and non-universal transport [11], log-periodic motion at high bias and large porosity [14]. Most of these studies deal with the motion of a single particle in a biased field. Instead, we consider the flow of a fluid of interacting particles through a percolating medium driven by concentration gradient (see below).

1.3 Concentration gradient

The mobile fluid constituents spread from high (toward the source end) to low particle concentration as the fluid flow from a source. The field caused by the concentration gradient drives the fluid constituents as described by the concentration diffusion equation (1) in a homogeneous space. Stream of particles emanating from the source execute their stochastic (random walk) motion. The instantaneous distribution of particles forms a special morphology. Particularly, the locus of the nearest neighbor particles on the moving fluid front, i.e., the profile of the concentration front, leads to the morphology of a percolating cluster at the percolation threshold. This is known as gradient percolation [18] since the dispersion and distribution of particles is caused by the concentration gradient. The shape of the concentration gradient is well known and the concentration of particles on the front provides a good estimate of the percolation threshold.

Evolution of the concentration profile of an interacting (nearest neighbor) lattice gas in a homogeneous space [19] seems consistent with the diffusion equation (1). In fact, the velocity of the front from eq. (1) can be used to calibrate the time and length scale of the lattice gas simulations to understand the diffusion of specific system such as chlorine [19]. Obviously the motion of the front depends on the shape of the concentration profile, i.e., the concentration gradient. How does the concentration profile change if the fluid moves through a percolating porous medium near its percolation threshold? How does the front speed depend on the porosity near the threshold?

Let us consider a finite system with the one end (bottom) connected to the fluid source (particles) and the opposite end (top) open. The fluid moves from bottom to top as driven by the concentration gradient. The fluid particles move from the source into the bottom and escape the system from the top. The concentration profile becomes stable as the system reaches the steady-state, i.e., when the in-flux (at the bottom) becomes equal to the out-flux (from the top). The steady-state concentration profile depends on porosity and we investigate the changes in profile as we vary the porosity near the threshold. Since the shape of the profile, i.e. the concentration gradient, provides the driving field, the motion of the front and the flux rate may depend on porosity as well. In this paper, we analyze some of these issues by a computer simulation model presented in next section (2) followed by

results and discussion (in section 3). The conclusion is provided in the last section 4.

2 Model

The host matrix is prepared on a simple-cubic $L \times L \times L$ lattice. The percolating porous medium of porosity p is generated by randomly distributing barriers, one at a site, on a fraction $p_b = 1 - p$ sites. The porosity is kept above the percolation threshold $p \geq p_c (\simeq 0.312)$ so that a spanning cluster of connected pore extends from one of the sample to another. One end of this sample say the bottom ($x = 0$) is connected to a source of fluid represented by mobile particles. The opposite end (top) is open so that the fluid particles entering the lattice at the bottom can escape from the top. Each pore site in the bottom layer is occupied by the mobile fluid particle (with one particle at a site, the excluded volume effect).

The fluid is modeled by an interacting lattice gas. In order to introduce interaction we assign an occupation variable (S) to each site. An empty pore site i is assigned $S_i = -1$ while a site i with a fluid particle $S_i = 1$ and with a barrier $S_i = 0$. We use the following interaction energy,

$$E = U \sum_{ij} S_i S_j \quad (3)$$

where the interaction strength U is set at unity in units of the Boltzmann constant (k_B). The summation is restricted to nearest neighbor sites in this simulation. The fluid-fluid repulsive and fluid-pore attractive interactions are thus considered. The fluid particles attempt to move to an empty neighbor in a randomly selected direction with a Boltzmann distribution as in the Metropolis algorithm at temperature T [20]. A periodic boundary condition is used along the transverse (y, z) directions and open condition along the longitudinal (x) direction: a fluid particle cannot move below the bottom plane while it can escape the system if it attempts to move above the top plane. As soon as a particle leaves the pore site at the bottom, it is occupied by another particle from the source. Thus a constant fluid concentration/density of unity is maintained in the bottom plane throughout the

simulation. An attempt to move each particles once is defined as one Monte Carlo step (MCS).

As the simulation proceeds, particles move out into the medium from the bottom, fluid spreads, and concentration profile evolves. The period during which none of the particles from the source reaches the top defines the unsteady ("short" time) regime. It is in this unsteady state regime that the lattice gas simulation seems to reproduce the results of continuum diffusion eq. (1) particularly the form of concentration profile and its motion in homogeneous space [19]. In the steady-state ("long" time) regime, the fluid-in-flux (at bottom) equals the fluid-out-flux (at the top), and the continuity equation for the conservation of the mass is satisfied, i.e.,

$$\nabla \cdot j = 0 \quad . \quad (4)$$

In the steady-state flow regime the concentration profile becomes stable. One can evaluate the fluid current density (j) along the longitudinal direction. We investigate the transport behavior of fluid (the center of mass) and its constituent particles, the tracers and the flux response. Simulations are carried out for a long time with many independent runs to obtain a reliable estimate of physical quantities, particularly near percolation threshold. Further, we have used different lattice sizes to check for significant finite size effects which are not detected in these data.

3 Results and Discussion

Simulations are performed on different lattice sizes to look for finite size effects with most data generated on 30^3 and 50^3 samples. The porosity is varied with $p \geq 0.312$. The temperature is constant $T = 2$ in units of Boltzmann constant. N_r independent samples, $N_r = 32 - 256$, are used via parallelization with MPI calls with up to five million time steps. We have analyzed the variation of the rms displacement of tracers and their center of mass with time, concentration profile, and flux rate density as a function of porosity near percolation threshold.

3.1 RMS Displacements

In section 1 we introduced the power-law dependence of the rms displacement (eq. 2) for a single particle executing its stochastic motion. The fluid consists of many particles (in our model) and the collective motion of the fluid (i.e., the center of mass) results from the motion of individual particles, the tracers. The rms displacement of tracer, R_t , and that of the center of mass, R_c , are described by the power-law dependence (eq. 2). Since the behavior of R_c describes the motion of the fluid, the center of mass of the particles and fluid will be used synonymously as far as the fluid motion is concerned. As the fluid enters the system from the bottom, the concentration gradient field drive the fluid from the bottom. The longitudinal (x -) component of the rms displacement is much larger than the transverse (y, z) components. The power-law behavior of the total rms displacement (for both tracer and center of mass of the fluid) is dominated by the longitudinal component. Figure 1 shows the variation of rms displacements for tracer with time at various porosities. The linear fit of data on a log-log scale in the short time regime ($10^2 - 10^4$ steps) suggest a power-law with exponent $\nu_1 \simeq 1/2$. In the long time (asymptotic regime), the power-law exponent becomes higher $\nu_2 \simeq 1$ leading to a drift-like motion. Such a crossover from diffusion to drift is clearly seen at relatively higher porosities ($p_s = 0.360, 0.400$). The crossover occurs at a characteristic time step (t_c) which increases on decreasing the porosity toward the threshold. The rms displacement of the center of mass also shows similar crossover behavior (figure 2).

The closer to the percolation threshold we are, the longer (t_c) it takes to reach the asymptotic power-law behavior of the rms displacements for the tracer and fluid. Particularly at $p = 0.312$, the lowest porosity we simulated near percolation threshold ($p_c \simeq 0.311608$) [7], it was difficult to reach long time power-law behavior with the larger samples. Therefore, we performed our simulation on a smaller sample (30^3) for 5×10^6 time steps. The variation of the longitudinal component of the rms displacement with time is presented in figure 3 which shows a clear crossover to drift in the long time regime. Further we note that the qualitative behavior for the variation of the rms displacement with time remain the same as that on the larger sample for both tracer and fluid.

It is worth pointing out that there are extensive computer simulations on biased diffusion with a variety of biased fields [11-17]. In most of these

studies the tracer's motion slows down at low porosity (closer to percolation threshold) and high bias as the bias competes with the barriers at the pore boundary. Thus there is no asymptotic drift behavior [15] of a biased random walk in a percolating medium near threshold at high biased field. In our driven system, the concentration gradient provides the bias. The gradient field varies (see below) as we vary the porosity, but the asymptotic drift behavior of the rms displacement of the tracer and fluid persists no matter how close we are to the percolation threshold. This implies that the bias generated by the concentration gradient, perhaps not too strong, is an effective method of transport through a porous medium.

3.2 Concentration profile

Initially, the concentration profile is a delta function at $x = 1$, since there is no fluid particle in the sample except in the bottom plane ($x = 1$) where each pore site is occupied by a fluid particle. As the simulation proceeds the fluid spreads and the profile changes. Figure 4 shows a typical evolution of the concentration profile. In the unsteady flow regime, i.e., when no fluid particle arrives at the top, the shape of the profile seems consistent with the concentration diffusion (eq. 1). In the long time (asymptotic) regime, the concentration profile becomes stable and the system reaches a steady-state flow (see below). The steady-state profile depends on porosity. Figure 5 shows the steady-state profile at various porosities above the percolation threshold. At low porosity ($p = 0.312$), we see a spatial variation in concentration gradient. A relatively linear gradient (dc/dx) develops at higher porosities. The gradient field (concentration gradient) is delicately controlled by porosity in such a way that the asymptotic drift motion of tracer and fluid occurs. The net transfer of fluid across the sample, i.e., the flow response, depends on porosity which is discussed in the following.

3.3 Flow response

Fluid enters the sample at the bottom ($x = 1$) and leaves from the top ($x = L$). There is a net fluid transfer (q) along x -direction. We evaluate

the current density (j) resulting from the rate of fluid (mass) transfer,

$$j = \frac{1}{L^2} \cdot \frac{dq}{dt} \quad (5)$$

In fact, we evaluate both, the input (bottom) and output (top) current densities (j) separately. Figure 6 shows the variation of these current (flux) densities at various porosities. As expected, the input flux density is higher and output flux density is lower initially, i.e. in the unsteady-flow regime. In steady-state, both must be equal, as seen in figure 6. Thus we see that the flow has reached the steady-state at nearly all porosities except very close to the percolation threshold ($p_s = 0.312$). Looking at the trend in data, it is easy to estimate the flux density by extrapolation. However, we have carried out our simulation for a long time on a smaller sample to achieve the steady state at $p_s = 0.312$; figure 7 shows the input and output flux density.

It would be interesting to quantify how the steady-state flux density (j) depend on porosity. Figure 8 shows the variation of j with porosity (p_s). We see a relatively good power-law dependence,

$$j \propto (\Delta p)^\beta \quad (6)$$

where $\Delta p = p_s - p_c$ and $\beta \simeq 1.7$. Fig. 8 shows that this effective exponent β increases with increasing L and thus asymptotically may be compatible with the exponent $\simeq 2$ of random resistor networks [3-6].

4 Conclusion

A computer simulation model is used to study the density profile and fluid flow through an open porous medium near the percolation threshold. The fluid is driven by the concentration gradient which is evolved from maintaining a constant concentration, unity at the source (bottom) and zero at the top. RMS displacements of tracer and fluid are studied in detail at various porosities near the percolation threshold. The long time asymptotic power-law behavior of the rms displacement $R \propto t$ is found at all porosities above the threshold unlike the biased diffusion in previous simulations [11-15]. We believe that such an asymptotic drift is achieved due to the concentration

gradient caused by a delicate competition between the stochastic motion of the fluid particles and the pore barriers. The shape of the density profile is sensitive to porosity.

We have shown that the fluid flux through such a percolating porous medium reaches a steady-state above the percolation threshold. The flux density (j) depends on porosity and we characterize it by an empirical power-law relation (eq. 6). We plan to study the effects of parameters such as temperature, pressure, etc. in such a gradient driven system.

Acknowledgment: This work is supported under ONR PE# 0602435N. This work was supported in part by a grant of computer time from the DOD High Performance Computing Modernization Program at the Major Shared Resource Center (MSRC), NAVO, Stennis Space Center.

References:

- [1] H.E. Stanley and J.S. Andrade Jr., *Physica A* 295, 17 (2001).
- [2] E.L. Cussler, "*Diffusion: Mass transfer in fluid systems*" (Cambridge University Press, 1984); C.A. Silebi and W.E. Schiesser, "*Dynamic Modeling of Transport Process Systems*" (Academic Press, Inc., 1992).
- [3] M. Sahimi, "*Flow and transport in Porous Media and Fractured Rock*" (VCH Weinheim, 1995).
- [4] D. Stauffer and A. Aharony, "*Introduction to Percolation Theory*", Second Edition (Taylor and Francis, 1994).
- [5] A. Bunde and S. Havlin, eds., "*Fractals and Disordered Systems*", Second Edition (Springer, New York, 1996).
- [6] M. Sahimi, "*Application of Percolation Theory*" (Taylor and Francis, 1994).
- [7] G. Paul, R.M. Ziff, and H.E. Stanley, *Phys. Rev. E* 64, 261151 (2001).
- [8] C.D. Lorenz and R.M. Ziff, *Phys. Rev. E* 57, 230 (1998).
- [9] D. Stauffer and R.M. Ziff, *Int. J. Mod. Phys. C* 11, 205 (2000).
- [10] S. Havlin and D. Ben Avraham, *Adv. Phys.* 36, 395 (1987).
- [11] R.B. Pandey, *Phys. Rev. B* 30, 489 (1984).
- [12] H. Boettger and V.V. Bryskin, *Phys. Stat. Sol. (b)* 113, 9 (1982).
- [13] M. Barma and D. Dhar, *J. Phys. C* 16, 1451 (1983).
- [14] D. Stauffer and D. Sornette, *Physica A* 252, 271 (1998).
- [15] D. Dhar and D. Stauffer, *Int. J. Mod. Phys. C* 9, 349 (1998).
- [16] E. Seifert and M. Sussenbach, *J. Phys. A* 17, L 703 (1994).
- [17] A. Bunde, S. Havlin, and H.E. Roman, *Phys. Rev. A* 42, 6274 (1990).
- [18] M. Rosso, B. Sapoval, and J.-F. Gouyet, *Phys. Rev. Lett.* 57, 3195 (1986); R.P. Wool, "*Polymer Interfaces*", Chapter 4 (Hanser Publishers, 1995).
- [19] R.B. Pandey, W. Wood, and J.G. Gettrust, Preprint (2001).
- [20] K. Binder, ed., "*The Monte Carlo Methods in Condensed Matter Physics*" Topics in Applied Physics, Vol. 71 (Springer-Verlag, 1995).

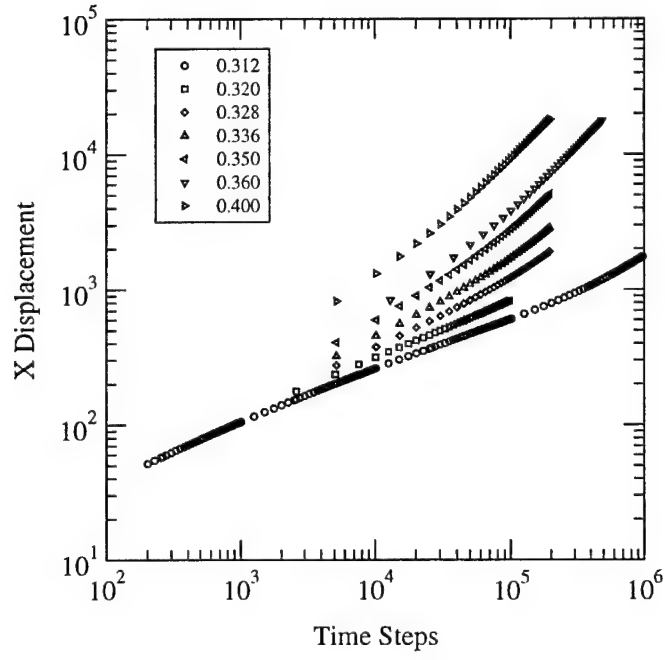


Figure 1: Root mean square (rms) displacement of the tracer with time steps on a log-log scale for various porosities, $p = 0.312 - 0.4$ on a 50^3 sample with $T = 2.0$. $N_r = 32 - 256$ independent samples.

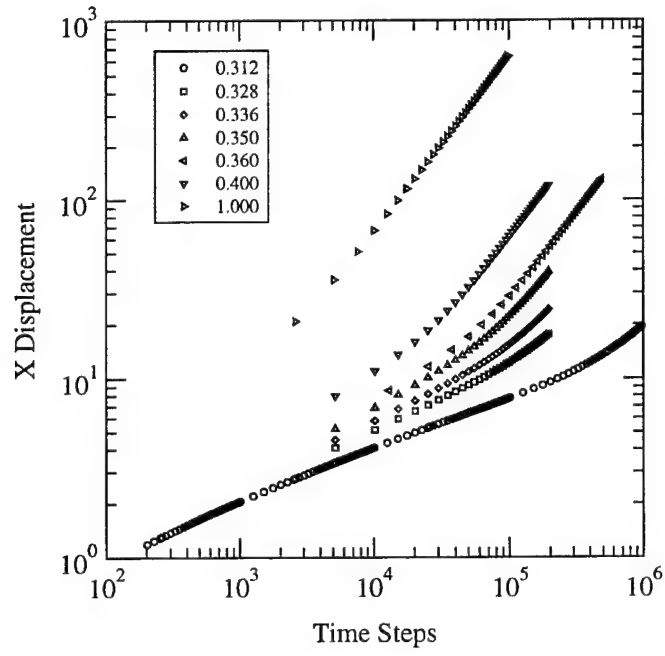


Figure 2: RMS displacement of the center of mass of the fluid particles with time steps. Statistics is the same as in figure 1.

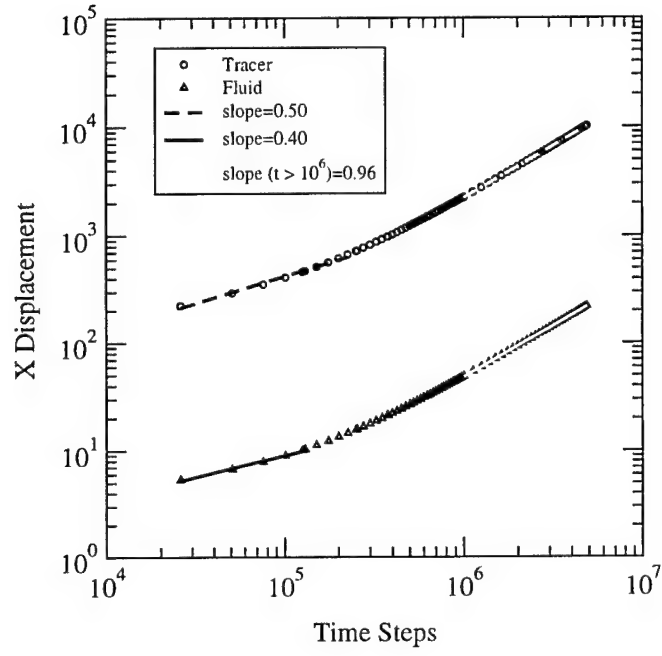


Figure 3: RMS displacement of the tracer and the center of mass versus time steps at $p = 0.312$ on a 30^3 sample with $N_r = 256$.

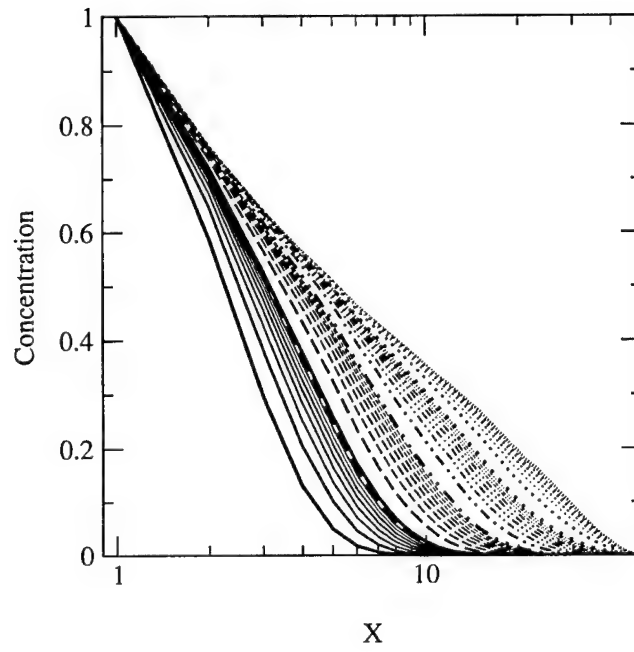


Figure 4: Evolution of concentration profile on a 50^3 sample at $p = 0.312$ with $N_r = 256$.

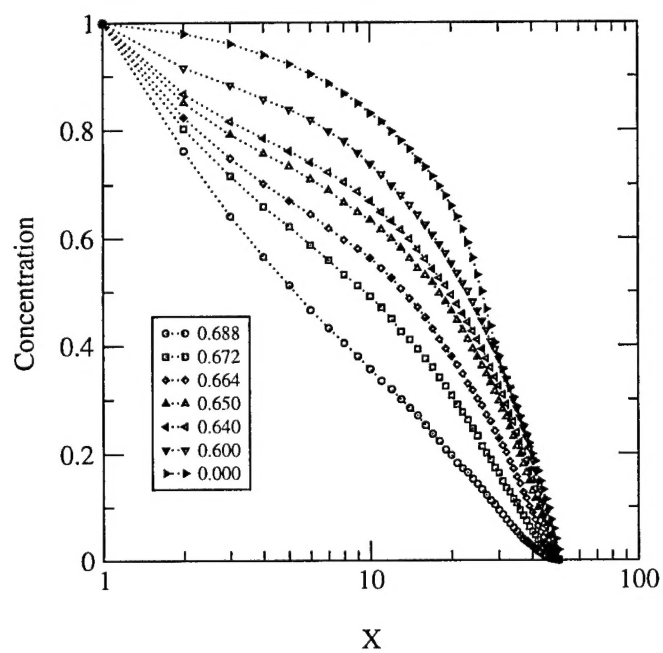


Figure 5: Concentration profile in steady-state. Statistics is the same as in figure 1.

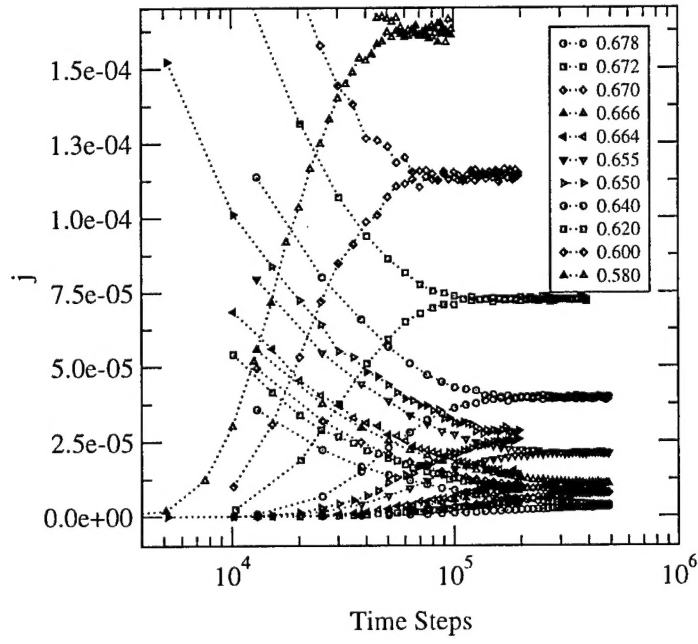


Figure 6: Flux rate density (j) versus time steps at various porosities. Statistics is the same as in figure 1. The top data is the flux-in at the bottom and bottom data is the flux-out from the top.

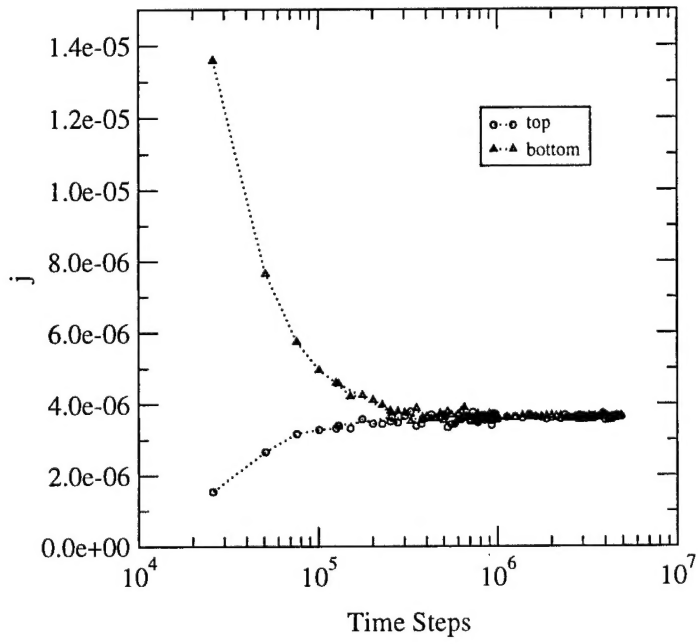


Figure 7: Flux rate density (j) versus time steps at $p = 0.312$ on a 30^3 sample with the same statistics as in figure 3.

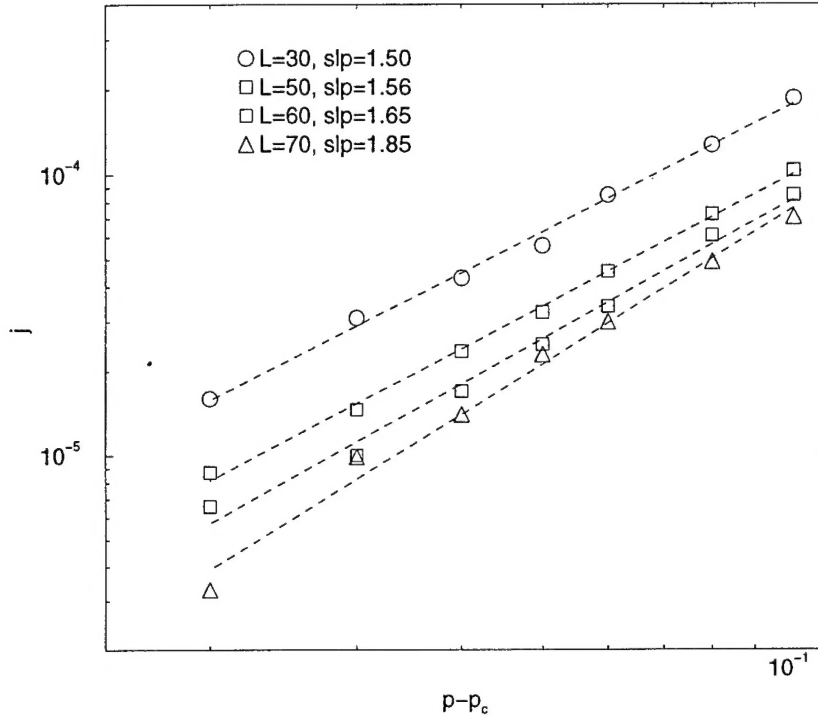


Figure 8: Log-log plot of j versus $p - p_c$ at $T = 1$ for $L = 30$ (\times), 50 ($+$), 60 (stars), and 70 (squares), with slopes 1.5, 1.6, 1.7, 1.75, respectively. We average over usually 8 lattices and 10^5 time steps. This flux rate density j varies as the concentration gradient $\propto 1/L$.